

**Are your MRI contrast agents cost-effective?**

Learn more about generic Gadolinium-Based Contrast Agents.



**FRESENIUS  
KABI**

caring for life

**AJNR**

**Proton MR Spectroscopy in Neonates with  
Perinatal Cerebral Hypoxic-Ischemic Injury:  
Metabolite Peak-Area Ratios, Relaxation  
Times, and Absolute Concentrations**

J.L.Y. Cheong, E.B. Cady, J. Penrice, J.S. Wyatt, I.J. Cox  
and N.J. Robertson

This information is current as  
of April 19, 2024.

*AJNR Am J Neuroradiol* 2006, 27 (7) 1546-1554  
<http://www.ajnr.org/content/27/7/1546>

ORIGINAL  
RESEARCH

J.L.Y. Cheong  
E.B. Cady  
J. Penrice  
J.S. Wyatt  
I.J. Cox  
N.J. Robertson

# Proton MR Spectroscopy in Neonates with Perinatal Cerebral Hypoxic-Ischemic Injury: Metabolite Peak-Area Ratios, Relaxation Times, and Absolute Concentrations

**BACKGROUND:** Results from cerebral proton  $^1\text{H}$ -MR spectroscopy studies of neonates with perinatal hypoxic-ischemic injury have generally been presented as metabolite peak-area ratios, which are T1- and T2-weighted, rather than absolute metabolite concentrations. We hypothesized that compared with  $^1\text{H}$ -MR spectroscopy peak-area ratios, calculation of absolute metabolite concentrations and relaxation times measured within the first 4 days after birth (1) would improve prognostic accuracy and (2) enhance the understanding of underlying neurochemical changes in neonates with neonatal encephalopathy.

**METHODS:** Seventeen term infants with neonatal encephalopathy and 10 healthy controls were studied at 2.4T at 1 (1–3) and 2 (2–4) (median [interquartile range]) days after birth, respectively. Infants with neonatal encephalopathy were classified into 2 outcome groups (normal/mild and severe/fatal), according to neurodevelopmental assessments at 1 year. The MR spectroscopy peak-area ratios, relaxation times, absolute concentrations, and concentration ratios of lactate (Lac), creatine plus phosphocreatine (Cr), *N*-acetylaspartate (NAA), and choline-containing compounds (Cho) from a voxel centered on the thalami were analyzed according to outcome group.

**RESULTS:** Comparing the severe/fatal group with the controls (significance assumed with  $P < 0.05$ ), we found that Lac/NAA, Lac/Cho, and Lac/Cr peak-area ratios increased and NAA/Cr and NAA/Cho decreased; Lac, NAA, and Cr T2s were increased; [Lac] was increased and [Cho], [Cr], and [NAA] decreased; and among the concentration ratios, only [Lac]/[NAA] was increased. Comparison of the normal/mild group with controls revealed no differences in peak-area ratios, relaxation times, or concentration ratios but decreased [NAA], [Cho], and [Cr] were observed in the infants with normal/mild outcome. Comparison of the normal/mild and severe/fatal groups showed increased Lac/NAA and Lac/Cho and decreased NAA/Cr and NAA/Cho peak-area ratios, reduced [NAA], and increased Lac T2 in the infants with the worse outcome.

**CONCLUSIONS:** Metabolite concentrations, in particular [NAA], enhance the prognostic accuracy of cerebral  $^1\text{H}$ -MR spectroscopy—[NAA] was the only measurable to discriminate among all (control, normal/mild, and severe/fatal outcome) groups. However, peak-area ratios are more useful prognostic indicators than concentration ratios because they depend on metabolite concentrations and T2s, both of which are pathologically modulated. Concentration ratios depend only on the concentrations of the constituent metabolites. Increased Cr T2 may provide an indirect marker of impaired cellular energetics, and similarly, NAA T2 may constitute an index of exclusively neuronal energy status. Our recommendation is to collect data that enable calculation of brain metabolite concentrations. However, if time constraints make this impossible, metabolite peak-area ratios provide the next best method of assigning early prognosis in neonatal encephalopathy.

Intrapartum hypoxia-ischemia in term infants remains an important cause of acute neonatal encephalopathy and permanent brain injury,<sup>1</sup> affecting approximately 2 per 1000 births in the developed world.<sup>2,3</sup> In the last 20 years, phosphorus ( $^{31}\text{P}$ ) and proton ( $^1\text{H}$ ) MR spectroscopy have enabled characterization of the timing and pattern of acute brain metabolite changes following perinatal hypoxia-ischemia.<sup>4–14</sup>

Clinical and experimental  $^{31}\text{P}$ -MR spectroscopy studies

have demonstrated a biphasic pattern of impaired cerebral energy generation as a consequence of transient hypoxia-ischemia.<sup>4,7,12,14–17</sup> The initial phase of energy generation impairment during hypoxia-ischemia (reduced phosphocreatine [PCr], adenosine triphosphate [ATP], and intracellular pH [ $\text{pH}_i$ ]) resolves on resuscitation but is followed by a delayed secondary phase of apparent energy failure, termed “secondary energy failure,” with characteristics similar to those found during transient hypoxia-ischemia but accompanied by a rise in brain  $\text{pH}_i$ .

$^1\text{H}$ -MR spectroscopy has shown that cerebral lactate (Lac) rises during hypoxia-ischemia but is rapidly cleared on resuscitation,<sup>18</sup> only to be followed by a secondary increase after 12–24 hours<sup>8,19</sup> because of renewed production of Lac in brain tissue rather than entry via the circulation.<sup>20</sup> In the basal ganglia, an increased Lac/total creatine (Cr; ie, creatine plus PCr) peak-area ratio provides an early indication of the severity of brain injury in neonates following perinatal hypoxia-isch-

Received August 30, 2005; accepted after revision November 30.

From the Department of Paediatrics and Child Health (J.L.Y.C., J.P., J.S.W.), University College London, London, UK; the Department of Medical Physics and Bio-Engineering (E.B.C.), University College London Hospitals NHS Trust, London, UK; Imaging Sciences Department (I.J.C.), Division of Clinical Sciences, Faculty of Medicine, Imperial College London, UK; and the Department of Obstetrics and Gynaecology (N.J.R.), University College London, London, UK.

Address correspondence to Nicola J. Robertson, MD, FRCPCH, PhD, Department of Obstetrics and Gynaecology, University College London, 86–96 Chenies Mews, London WC1E 6HX, United Kingdom; e-mail: rmj@ucl.ac.uk

emia, before changes are apparent on conventional longitudinal and transverse relaxation time (T1 and T2, respectively)-weighted MR imaging. A number of groups have shown that Lac/Cr, Lac/N-acetylaspartate (NAA), or Lac/choline-containing compounds (Cho) peak-area ratios provide accurate prognostic markers of the severity of brain injury and subsequent neurodevelopmental outcome.<sup>5,8-10,11-12,21-23</sup> Indeed, such ratios may be more accurate than diffusion-weighted imaging (DWI) and the apparent diffusion coefficient (ADC) of brain water in assessing injury severity.<sup>21,22,24,25</sup> Although Lac peak-area ratios apparently give an accurate prognosis, there is no consensus on the most appropriate ratio to use. For example, up to 10 days following birth, increased Lac/Cr,<sup>11,12,22</sup> Lac/NAA,<sup>8-9</sup> and Lac/Cho<sup>5,10,21,23</sup> have all been described in neonates with subsequent poor neurodevelopmental outcome and evaluated as prognostic indices.

Few studies have measured absolute metabolite concentrations, expressed as millimole per kilogram wet weight of brain tissue because more complicated data-collection protocols and longer acquisition times are required.<sup>5,8-12,26,27</sup> Although peak-area ratios provide a useful prognostic guide in the first 2 weeks following birth in neonates with neonatal encephalopathy, peak-area ratios can be influenced by a number of factors, including changes in metabolite concentrations and relaxation times. Experimental perinatal hypoxia-ischemia studies have demonstrated increased metabolite T2s during secondary energy failure,<sup>28</sup> and these have been confirmed in neonatal encephalopathy.<sup>29</sup> It has also been shown that the apparent Cr T2 depends on the relative concentrations of creatine and PCr, which may alter during secondary energy failure.<sup>30</sup> Furthermore, a peak-area ratio could change as a result of a pathologic alteration in the concentration of either of the metabolites involved. It is, therefore, possible that interpretations based on peak-area ratios may be blind to additional pathologically important MR spectroscopy features.<sup>29,31-35</sup>

We hypothesized that compared with the interpretation provided by <sup>1</sup>H-MR spectroscopy peak-area ratios, metabolite absolute concentrations and relaxation times measured within the first 3–4 days after birth would (1) improve prognostic accuracy and (2) enhance the understanding of underlying neurochemical changes in infants with neonatal encephalopathy.

## Subjects and Methods

### Subjects

Ethical permission was granted by the University College London Committee on the Ethics of Human Experimentation. Informed parental consent was obtained for every examination.

Seventeen neonates with a mean ( $\pm$ SD) gestational age (GA) of 39.0 ( $\pm$ 1.6) weeks and a birth weight of 3.34 ( $\pm$ 0.45) kg were studied at a median (interquartile range) age of 1 (1–3) days. These neonates had clinical histories consistent with neonatal encephalopathy, which included an altered conscious state, abnormal tone and reflexes, seizures, and poor feeding. Neonatal encephalopathy severity was graded by using Sarnat scores<sup>36</sup>: 5 neonates had stage I; 5, stage II; and 7, stage III. In 5 deliveries, there was cord prolapse or placental abruption. Ten neonates had a 1-minute Apgar score of less than 5, 12 infants had metabolic acidosis (pH < 7.1 and/or base deficit > 12 mmol/L) in umbilical cord or arterial blood within 30 minutes of

birth, and all neonates with neonatal encephalopathy required resuscitation at birth. Infants with major congenital malformations and metabolic or known infective diseases were excluded from the study.

Ten healthy control neonates of GA 39.0 ( $\pm$ 1.8) weeks and birth weight 3.16 ( $\pm$ 0.53) kg comparable to those of the neonates with neonatal encephalopathy were recruited from the postnatal ward and studied at 2 (2–4) days. They had no history of perinatal hypoxia-ischemia or other significant illness. Controls had Apgar scores of  $\geq$ 9 at 1 minute and cord pH  $\geq$  7.31 (only available in 4 infants), and none required resuscitation. All control infants were physically and neurologically healthy at birth.

### Neurodevelopmental Assessment

All neonates with neonatal encephalopathy who survived were examined at 1 year with the modified Amiel-Tison neurologic assessment<sup>37</sup> and Griffiths developmental quotient (DQ).<sup>38</sup> They were classified into 2 outcome groups: severely abnormal/fatal outcome, which comprised neonates who had died as a direct consequence of neonatal encephalopathy ( $n = 4$ ) and those who had major impairment with disability on neurologic assessment and/or DQ < 75 ( $n = 3$ ); and those with normal/mildly abnormal outcome ( $n = 10$ ), who had either normal neuromotor outcome or mild abnormality on neurologic assessment.

### Patient Handling

<sup>1</sup>H-MR spectroscopy was performed either during natural sleep or after sedation with oral or rectal chloral hydrate (50–75 mg/kg). Neonates were studied in a protective perspex pod with gentle head restraint. Throughout the examination, neonates were monitored by using MR-compatible pulse oximetry and electrocardiogram and supervised by an experienced neonatal pediatrician trained in clinical MR imaging safety.

### MR Spectroscopy Methods

<sup>1</sup>H-MR spectra were obtained by using a 2.4T Bruker Avance system (Bruker Medizintechnik, Ettlingen, Germany) with a 40-cm clear bore, <sup>1</sup>H radio-frequency (RF) 100.3 MHz, actively shielded gradients (Bruker S-260), and a custom-made Helmholtz head coil of 15-cm diameter and length.<sup>39</sup> Localized <sup>1</sup>H metabolite and water spectra were obtained by using point-resolved spectroscopy (PRESS). There was a fixed delay of 7.6 ms (much less than the echo time [TE]) between the 90° RF pulse and the first 180° pulse, thereby optimizing sensitivity for Lac. With the neonate supine, cubic 8-mL voxels were positioned. First, an axial image was obtained; then an orthogonal medial sagittal section was positioned by using the axial image; and finally, by using the sagittal image, we centered the PRESS voxel on the thalami and the midline (Fig 1). Some signal-intensity inhomogeneity was apparent on the scout images, especially anteriorly. This was due to the Helmholtz coil, which, although giving a signal intensity-to-noise ratio (SNR) of approximately 70% greater than that provided by the standard Bruker birdcage coil,<sup>39</sup> had significantly poorer RF homogeneity. However, as PRESS RF pulse amplitudes were optimized while monitoring water signal intensity exclusively from the selected voxel which was much smaller than the Helmholtz coil, accurate 90° and 180° pulse flip angles were achieved throughout the MR spectroscopy voxel. The water signal intensity was suppressed by 3 chemical shift selection suppression (CHESS) pulses, each followed by “spoiler” magnetic-field gradient pulses.

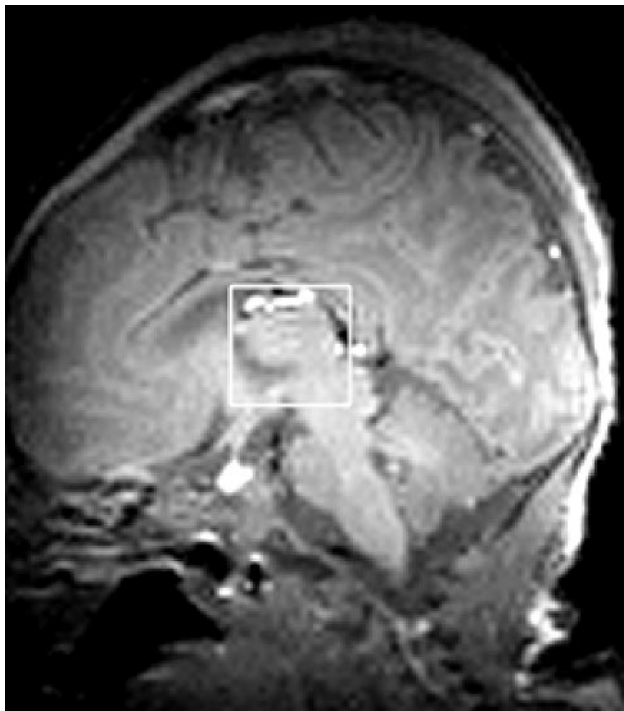


**Fig 1.** Voxel positioning. An axial scout image was obtained and an orthogonal medial sagittal section positioned (A); the 8-mL cubic PRESS voxel was then centered on the thalami and the midline by using the sagittal image (B).

### Absolute Quantitation Protocol

The absolute quantitation protocol consisted of the acquisition first of 3 partially relaxed spectra with repetition time (TR) of 2 seconds; TE 135, 270, and 540 ms; and 128, 128, and 256 summed echoes, respectively. These were followed by an essentially fully relaxed spectrum (TE, 270 ms; TR, 5 seconds; 128 summed echoes). Finally 6 non-water-suppressed fully relaxed spectra were collected (TE, 25, 270, 540, 1000, 1500, and 2000 ms; TR, 10 seconds; 8 summed echoes). Hence, the total acquisition time for the protocol (not including coil-tuning, scout imaging, voxel setup, and shimming) was about 40 minutes.

### Spectrum Analysis

Echoes were baseline-corrected and exponentially filtered (1-Hz line broadening) and then zero-filled before fast-Fourier transformation. Metabolite spectra had manual phasing (0th and 1st order) and then cubic spline baseline correction. Water spectra were also manually phased (0th order only) and had linear baseline correction. Peak areas were obtained by fitting Lorentzian profiles to the spectra by using  $\chi^2$  minimization with prior knowledge: starting chemical shifts, peak widths, and amplitudes; and for the Lac methyl doublet, J-coupling and equal component amplitudes.

Lorentzians are solutions of the Bloch equations and should be the true line shape.<sup>40</sup> They provided acceptable fits to Cho, Cr, and NAA. However, there was some deviation toward the base of the Lac methyl doublet, particularly when Lac was increased (Fig 2B, -C). Other researchers have used Gaussian functions, chosen empirically because they appeared to fit better. However, Cho, Cr, NAA, and Lac overlap numerous other resonances, many of which are phase-modulated multiplets with phase-inverted components at TEs of 135–540 ms. Hence, neither Lorentzians nor Gaussians provide optimal fits when other unresolved and phase-modulated components are present.

(State-of-the-art analysis methods, such as AMARES,<sup>41</sup> use exponentially decaying sinusoids [the time-domain equivalents of Lorentzians] to model the free-induction decay and, hence, will also be subject to this problem.)

Lac methyl doublet PRESS phase modulation presents a further problem (inversion at TE ~135 ms; rephased at ~270 ms and ~540 ms). Recent work suggests 144, 288, and 576 ms give more exact phase inversion and rephasing.<sup>42</sup> However, our results were obtained as part of a long-term study, and for consistency, TEs of 135, 270, and 540 ms were used throughout. Consequently, phase-inversion at a TE of 135 ms and rephasing at TEs of 270 and 540 ms may have been incomplete, further contributing to the slightly inexact Lorentzian fit. Again, this problem would exist regardless of the fitting function. Chemical shift artifact (spatial shift of the Lac methyl voxel relative to the methene) could have caused further incomplete phase modulation.<sup>43</sup>

### Peak-Area Ratios

Lac/Cr, Lac/NAA, Lac/Cho, NAA/Cr, NAA/Cho, and Cho/Cr were measured from the TE 270 ms, TR 2 seconds spectrum.

### Metabolite and Brain-Water Relaxometry

Cho, Cr, and NAA T2s were calculated, assuming monoexponential decay by using the TE 135, 270, and 540 ms spectra with a TR of 2 seconds. Incomplete phase modulation resulted in reduced Lac signal intensity with a TE of 135 ms, and hence, Lac T2 was determined by using only the TE 270 and 540 ms spectra. Because of the proximity of the lateral and third ventricles, it was possible that the PRESS voxel contained some CSF. Hence, brain-water T2 was determined by separating the signal intensity amplitudes of brain water and CSF by using a multi-TE method as described in this article.

Metabolite T1s were determined by comparing the signal-intensity amplitudes from the TE 270 ms spectra acquired with TRs of 2 and 5 seconds.

### The Brain-Water Internal Concentration Reference

Brain-water was used as an internal concentration reference.<sup>29,35</sup> To directly compare the brain metabolite signal intensity with that from brain-water, we separated the brain- and CSF-water signals. The brain-water signal intensity (T2 ~ 150 ms) was partitioned from that of CSF (T2 ~ 1 second) by fitting the double-exponential function  $S_{H_2O,b}(0) \exp(-TE/T_{2,b}) + S_{H_2O,CSF}(0) \exp(-TE/T_{2,CSF})$  to the non-suppressed multi-TE water peak areas by least-squares  $\chi^2$  minimization.  $S_{H_2O,b}(0)$  and  $S_{H_2O,CSF}(0)$  were the signal-intensity amplitudes of the required brain- and CSF-water components extrapolated to TE 0 ms, and  $T_{2,b}$  and  $T_{2,CSF}$  their respective relaxation times.

### Quantitation of Metabolite Concentrations

Metabolite concentrations (millimole/kilogram wet tissue) were determined by comparing the T2-corrected peak areas from the fully relaxed spectrum (TE, 270 ms; TR, 5 seconds), with the fully relaxed (TR, 10 seconds) partitioned brain-water signal intensity from the same voxel and an assumed brain-water concentration. The latter was derived from previously published data for postmortem infant whole-brain:  $[H_2O_b] = 556.0 [94.7 - 0.17 \text{ GPA}] \text{ mmol/kg wet weight}$  (where GPA is the gestational plus postnatal age in weeks).<sup>44</sup> For control infants, metabolite concentrations were calculated by using mean metabolite T2s determined from the whole group. For neonates with neonatal encephalopathy, concentrations were derived by using the metabolite T2s measured at each study. The small CSF voxel fraction in our study and the low CSF Lac concentrations reported in

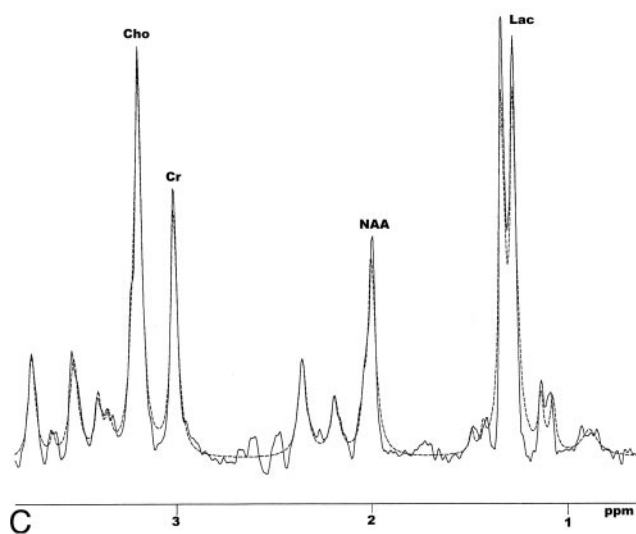
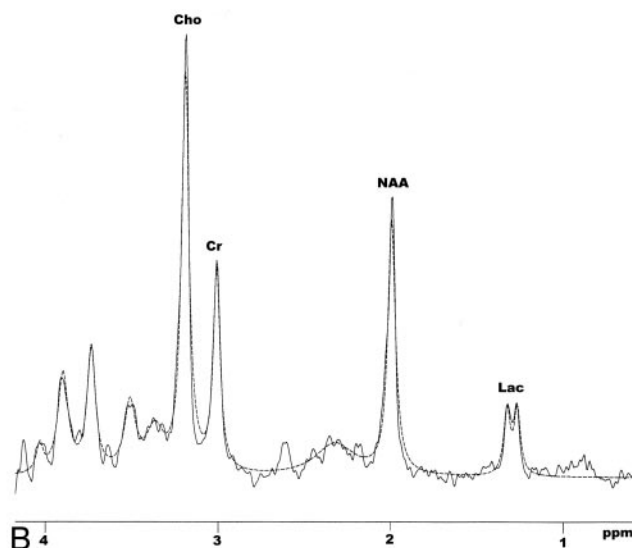
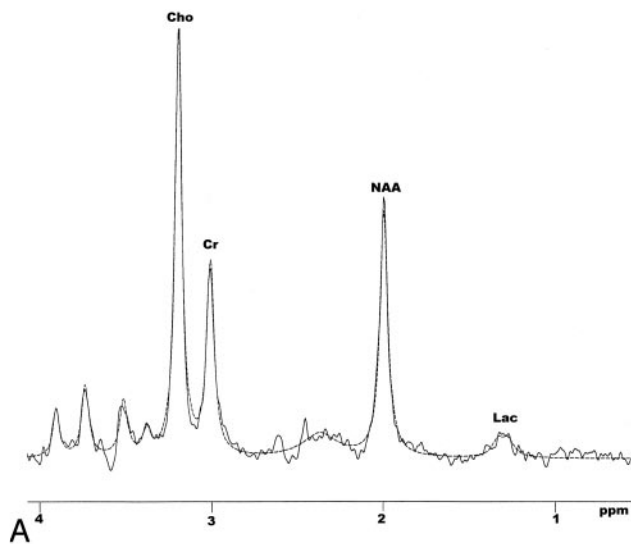


**Fig 2.** Representative brain spectra from a control infant and 2 neonates with neonatal encephalopathy acquired from an 8-mL voxel centered on the thalami by using PRESS (TE, 270 ms; and TR, 2 seconds). The dashed lines are the spectrum analysis Lorentzian profiles fitted to the peaks. *A*, Control. *B*, Normal/mild outcome. *C*, Severe/fatal outcome.

healthy adults and a neonatal encephalopathy subject (see Discussion) made it unnecessary to correct measured brain Lac concentrations for CSF Lac.

### Data Analysis

Data between groups were compared with *t* tests or Mann-Whitney rank sum tests as appropriate. The level of significance was  $P \leq .05$ .

## Results

### CSF

CSF voxel fractions were similar in the 3 groups of neonates: controls (mean [SD]), 5.0 (5.0%); normal/mild, 3.9 (4.5%); severe/fatal, 6.1 (6.0%); and all neonates, 4.9 (5.0%). As a consequence of the small CSF voxel fraction, the CSF T2 (1.67 [0.72] seconds) was difficult to measure and had a large SD.

### Metabolite Peak-Area Ratios

In neonates with neonatal encephalopathy with severe/fatal outcome, Lac/Cho, Lac/Cr, and Lac/NAA were all increased compared with control values, and Lac/NAA and Lac/Cho were increased compared with those in infants with nor-

mal/mild outcome (Table 1). In addition, NAA/Cr and NAA/Cho in the severe/fatal outcome group were reduced compared with both control and normal/mild groups.

### Metabolite T1 Relaxation

There were no significant differences in T1 relaxation between the outcome groups or between the outcome groups and controls (Table 2).

### Metabolite T2 Relaxation

Lac, NAA, and Cr T2 were increased in the group with severe/fatal outcome compared with the control group (Table 3). Lac T2 was increased in the severe/fatal outcome group compared with that of the normal/mild outcome group. No T2 differences were found for Cho or brain water.

### Metabolite Absolute Concentrations

The infants with a severe/fatal outcome showed elevated [Lac] and decreased [NAA], [Cho], and [Cr], compared with those of the control group, and lower [NAA], compared with those with a normal/mild outcome (Table 4). Neonates with neonatal encephalopathy with a normal/mild outcome also had decreased [NAA], [Cho], and [Cr], compared with those of the control group.

### Metabolite Concentration Ratios

The only difference was in [Lac]/[NAA], which was elevated in the neonates with neonatal encephalopathy with a severe/fatal outcome, compared with that in the control group (Table 5).

## Discussion

### Comparative Prognostic Efficacies

The results of our study suggest that metabolite concentrations, in particular [NAA], are the most accurate of the MR spectroscopy measurables in neonatal encephalopathy for assigning prognosis (Tables 1–5). However, metabolite peak-

**Table 1: Metabolite peak-area ratios for Lac/Cr, Lac/NAA, Lac/Cho, NAA/Cr, NAA/Cho, and Cho/Cr**

Metabolite Ratio	Control Group (n = 10)	Neonatal Encephalopathy Group (n = 17)		P Values		
		Normal/Mild Outcome (n = 10)	Severe/Fatal Outcome (n = 7)	Control Versus Normal/Mild Outcome	Control Versus Severe/Fatal Outcome	Normal/Mild Outcome Versus Severe/Fatal Outcome
Lac/Cr	0.38 (0.10)	0.41 (0.13)	0.70 (0.45–2.65)	.61	.04*	.06
Lac/NAA	0.24 (0.06)	0.29 (0.09)	0.54 (0.35–2.66)	.11	.02*	.03*
Lac/Cho	0.15 (0.03)	0.19 (0.05)	0.32 (0.22–1.26)	.06	.02*	.04*
NAA/Cr	1.59 (0.19)	1.41 (0.28)	1.16 (0.14)	.09	<.001*	.04*
NAA/Cho	0.66 (0.08)	0.67 (0.09)	0.56 (0.11)	.73	.04*	.04*
Cho/Cr	2.47 (0.57)	2.10 (0.31)	2.12 (0.36)	.09	.17	.91

**Note:**—Lac indicates lactate; NAA, *N*-acetylaspartate; Cho, choline; Cr, creatine.

\* Denotes statistically significant differences between the groups. Values are mean (SD) and median (interquartile range) as appropriate.

**Table 2: Spin-lattice relaxation times (T<sub>1</sub>; s) of Lac, NAA, Cho, and Cr**

Metabolite	Control Group (n = 10)	Neonatal Encephalopathy Infants (n = 17)		P Values		
		Normal/Mild Outcome (n = 10)	Severe/Fatal Outcome (n = 7)	Control Versus Normal/Mild Outcome	Control Versus Severe/Fatal Outcome	Normal/Mild Outcome Versus Severe/Fatal Outcome
Lac	1.28 (0.44)	1.39 (0.63)	1.28 (0.56)	.68	1.00	.72
NAA	1.31 (0.31)	1.27 (0.12)	1.16 (0.14)	.52	.26	.09
Cho	1.18 (0.22)	1.13 (0.16)	1.11 (0.18)	.62	.53	.78
Cr	1.66 (0.64)	1.27 (1.22–1.39)	1.22 (0.23)	.65	.11	.46

**Note:**—Lac indicates lactate; NAA, *N*-acetylaspartate; Cho, choline; Cr, creatine. Values are mean (SD) and median (interquartile range) as appropriate.

**Table 3: Spin-spin relaxation times (T<sub>2</sub>; ms) of Lac, NAA, Cho, and brain water**

Metabolite	Control Group (n = 10)	Neonatal Encephalopathy Infants (n = 17)		P Values		
		Normal/Mild Outcome (n = 10)	Severe/Fatal Outcome (n = 7)	Control Versus Normal/Mild Outcome	Control Versus Severe/Fatal Outcome	Normal/Mild Outcome Versus Severe/Fatal Outcome
Lac	221.8 (196.3–287.7)	242.8 (226.1–300.5)	380.5 (272.3–417.5)	.43	.04*	.01*
NAA	368.9 (68.1)	383.6 (85.8)	490.6 (155.1)	.68	.04*	.09
Cho	383.6 (84.2)	408.0 (114.8)	433.2 (40.6)	.59	.17	.41
Cr	199.2 (192.4–225.3)	234.6 (212.4–254.2)	259.7 (29.6)	.10	<.001*	.13
Brain water	164.9 (19.3)	157.0 (20.4)	144.9 (32.3)	.38	.13	.36

**Note:**—Lac indicates lactate; NAA, *N*-acetylaspartate; Cho, choline; Cr, creatine.

\* Denotes statistically significant differences between the groups. Values are mean (SD) and median (interquartile range) as appropriate.

**Table 4: Absolute concentrations (mmol/kg wet weight) of Lac, NAA, Cho, and Cr**

Metabolite	Control Group (n = 10)	Neonatal Encephalopathy Infants (n = 17)		P Values		
		Normal/Mild Outcome (n = 10)	Severe/Fatal Outcome (n = 7)	Control Versus Normal/Mild Outcome	Control Versus Severe/Fatal Outcome	Normal/Mild Outcome Versus Severe/Fatal Outcome
Lac	2.78 (0.83)	3.24 (1.25)	4.60 (3.20–12.08)	.34	.01*	.11
NAA	9.21 (1.29)	7.72 (1.46)	5.24 (2.58)	.03*	<.001*	.03*
Cho	4.39 (0.78)	3.62 (0.52)	2.60 (2.30–3.80)	.02*	.02*	.14
Cr	10.94 (1.88)	9.07 (2.12)	7.93 (3.39)	.05*	.03*	.41

**Note:**—Lac indicates lactate; NAA, *N*-acetylaspartate; Cho, choline; Cr, creatine.

\* Denotes statistically significant differences between the groups. Values are mean (SD) and median (interquartile range) as appropriate.

area ratios, which are relaxation-weighted, are more useful prognostic indicators than relaxation times or concentration ratios. For example, whereas Lac/Cr and Lac/Cho peak-area ratios were increased in the neonatal encephalopathy group with severe/fatal outcome compared with both the control and

normal/mild groups, there were no differences in [Lac]/[Cr] or [Lac]/[Cho].

Our Lac/Cr, Lac/Cho, Lac/NAA, NAA/Cr, and NAA/Cho peak-area ratios are consistent with previously published data<sup>8–12</sup> and confirm the important role of <sup>1</sup>H-MR spectroscopy

**Table 5: Concentration ratios involving Lac, NAA, Cho, and Cr**

Concentration Ratio	Neonatal Encephalopathy Infants ( <i>n</i> = 17)			<i>P</i> Values		
	Control Group ( <i>n</i> = 10)	Normal/Mild Outcome ( <i>n</i> = 10)	Severe/Fatal Outcome ( <i>n</i> = 7)	Control Versus Normal/Mild Outcome	Control Versus Severe/Fatal Outcome	Normal/Mild Outcome Versus Severe/Fatal Outcome
[Lac]/[Cr]	0.26 (0.09)	0.33 (0.11)	0.68 (0.28–2.32)	.12	.11	.26
[Lac]/[NAA]	0.31 (0.12)	0.39 (0.13)	0.69 (0.38–4.12)	.19	.05*	.09
[Lac]/[Cho]	0.66 (0.26)	0.83 (0.30)	2.33 (0.73–4.81)	.19	.06	.22
[NAA]/[Cr]	0.86 (0.15)	0.81 (0.73–0.94)	0.72 (0.14)	.79	.08	.09
[NAA]/[Cho]	2.12 (0.28)	2.14 (0.34)	1.90 (1.35–2.08)	.89	.16	.34
[Cho]/[Cr]	0.41 (0.08)	0.42 (0.11)	0.40 (0.33–0.43)	.82	.81	.88

**Note:**—Lac indicates lactate; NAA, *N*-acetylaspartate; Cho, choline; Cr, creatine.

\*Denotes statistically significant differences between the groups. Values are mean (SD) and median (interquartile range) as appropriate.

in assigning an early prognosis of neonates with neonatal encephalopathy. Indeed, previous studies have shown that compared with qualitative or quantitative DWI, MR spectroscopy peak-area ratios were better prognostically in term infants with encephalopathy. Qualitative DWI underestimated injury extent, whereas proton MR spectroscopy on the first day after birth was predictive of outcome.<sup>24</sup> At age 1–10 days, Lac/Cho in deep gray matter was predictive, whereas brain-water ADC was not.<sup>21</sup>

Our study showed very sensitive outcome prediction provided by the [NAA]. A preliminary study on metabolite concentrations in neonates with neonatal encephalopathy documented increases in [Lac] and reductions in [NAA], [Cho], and [Cr], similar to those reported here<sup>29</sup>; however, there were fewer infants than in the present study and limited neurodevelopmental follow-up.

Our ideal recommendation for prognosis is to measure brain metabolite concentrations. However, if time constraints or limited MR system capabilities make this procedure impossible, metabolite peak-area ratios provide the next best method of assigning early prognosis in neonatal encephalopathy.

#### Peak-Area and Concentration Ratio Interpretation

Although peak-area ratios are prognostically useful, our observed changes in metabolite concentrations and T2s suggest that interpretation requires caution. Pathologic changes in the concentrations and relaxation times of individual metabolites are not deducible from peak-area or concentration ratios. For example, because both the NAA and Cho concentrations and T2 relaxation are altered in neonates with neonatal encephalopathy, a fall in NAA/Cho peak-area ratio should not automatically lead the investigator to conclude that [NAA] has decreased or to estimate the magnitude of such fall. Absolute quantitation of metabolites can assess precise changes in [NAA] and [Cho], allowing a more accurate interpretation of pathologic sequelae. In particular, our quantitative results demonstrate that Cr does not constitute a stable reference for peak-area ratios. Compared with that of controls, the absolute concentration of Cr was reduced in both the normal/mild and severe/fatal outcome groups and Cr T2 was significantly increased in the latter group.

#### Relaxation Times

Lac, NAA, and Cr T2 were increased in the group with severe/fatal outcome compared with those in the control group. Metabolite and brain-water T2s increase in experimental models following transient hypoxia-ischemia<sup>28,45,46</sup> and in neonates with neonatal encephalopathy.<sup>29</sup> Our observed increase in Cr T2 in the severe/fatal outcome group would have caused pathologic modulation of Cr peak-area ratios. The increase may have resulted from 2 factors: PCr hydrolysis, leading to increased creatine and increased intracellular water, resulting in motional T2 lengthening.

The 2 major components of the Cr peak (PCr and creatine) have different T2 values (143 ms and 297 ms, respectively<sup>30</sup>). Substantial PCr hydrolysis to creatine during hypoxia-ischemia, and possibly also during secondary energy failure, would result in an apparent increase in the composite Cr T2, which, under conditions of constant Cr concentration, would increase the Cr resonance amplitude and reduce all peak-area ratios referenced to Cr. Indeed, experimental studies have shown that the T2s of Cho, Cr, NAA, and Lac all increase during both transient hypoxia-ischemia and secondary energy failure and that during secondary energy failure, these increases correlate with falling cerebral nucleotide triphosphate (mainly ATP) levels.<sup>28</sup> A likely consequence of reduced ATP is failure of the ATP-dependent Na<sup>+</sup>/K<sup>+</sup> pump, resulting in water influx, reduced cytosolic viscosity, and increased molecular mobility, leading to T2 lengthening.<sup>47</sup> On the grounds of its dependence on both PCr hydrolysis and ATP levels, Cr T2 may thus be considered an indirect probe of energy metabolism.

#### Study Limitations

Possible limitations of our study include the time taken to acquire the data from each infant (~40 minutes), the spatial resolution of the voxel (8 mL), and the use of a single voxel. However, if the infant is stable, then the length of examination is acceptable, considering the wealth of information obtained. The choice of voxel volume was directed by a desire to maximize SNR and spectrum resolution concomitant with acquiring data only from a limited brain region susceptible to hypoxic-ischemic injury. This choice was particularly important because the NAA concentration in neonatal brain is lower than that in adults. In addition, the NAA concentration was very low in severe neonatal encephalopathy, and because the

protocol included a TE of 540 ms, we required an 8-mL voxel to collect data with sufficient SNR.

### **Intravoxel CSF Determination**

We have not compared our CSF voxel fractions with estimates obtained from conventional MR imaging CSF/brain partitioning, first because our localized MR spectroscopy CSF fractions are essentially whole-voxel averages. Hence, to compare with conventional MR imaging, we would have to obtain many closely spaced parallel image sections covering the whole voxel. We were not able to include such an acquisition during the limited scan time available. Furthermore, a single such study would not provide statistical power for comparison. Second, the ability to separate CSF and brain-tissue pixels in conventional MR imaging is based on differences in their signal intensity amplitude, which, in turn, depend on differences in relaxation time. Hence, MR spectroscopy 2-component partitioning based on CSF and brain-water T2 and MR imaging signal intensity–amplitude partitioning are essentially founded on similar principles and should give comparable results.

Our brain-water and CSF T2 measurements justified a 2-component fit when separating CSF signal intensity from that of brain. The thalamus-centered voxel contained mainly gray matter and had an overall T2  $\sim$  155 ms (Table 3). In previous studies of neonatal brain using an occipitoparietal voxel (predominantly unmyelinated white matter), we measured T2  $\sim$  223 ms.<sup>35</sup> The similarity of the thalamus-centered and occipitoparietal T2s compared with the much longer CSF T2 ( $\sim$  1.7 seconds) justified fitting only a single brain component when estimating the CSF voxel fraction.

### **Lactate Contamination**

There are 2 possible sources of MR spectroscopy signal-intensity contamination that may have resulted in overestimation of the intracellular Lac concentration. In cases of severe injury leading to significant cell death, membrane breakdown products may contribute to the Lac resonance. However, the spectrum displayed in Fig 2C (TE, 270 ms) exhibits no resonance at  $\sim$  1.6 ppm and only a small resonance at  $\sim$  0.9 ppm. If substantial liberation of fatty acids had occurred at the early stage of cerebral injury in our study, significant  $-\text{CH}_2\text{CH}_2\text{CO}-$  and  $-\text{CH}_3$  signals would have been seen at these respective chemical shifts.<sup>48</sup> As a consequence of these observations, contamination of the Lac methyl resonance by signal intensity from lipid  $-(\text{CH}_2)_n-$  protons was probably insignificant in our studies.

CSF Lac may also be a potential contaminant. In healthy adults, CSF Lac is 0.8–2.4 mmol/L.<sup>49–51</sup> In neonatal encephalopathy, CSF Lac concentration may be higher and was 3.7 mmol/L in a severely affected infant in the present study.<sup>52</sup> Both CSF Lac concentration and T2 may vary unpredictably pathologically; therefore, without knowledge of these at the time of study, it is impossible to rigorously correct apparent brain Lac concentrations for CSF contamination. However, approximate estimations can be made. Assuming CSF Lac T2  $\approx$  brain Lac T2 (the former is probably longer), 4.9% CSF fraction (the mean for all infants in our study), and 2.4 mmol/L CSF Lac, we believe that the apparent Lac concentration would overestimate the true brain value by  $\sim$  0.12

mmol/L. Assuming the largest CSF fraction measured (19.2%) and 3.7 mmol/L CSF Lac, we believe that the apparent Lac concentration would overestimate the true brain value by  $\sim$  0.88 mmol/L. In conclusion, the effect of CSF Lac was, at the most, comparable to random error and, in general, much smaller.

### **Interpretation of Metabolite Concentrations and T2s**

Our metabolite concentration and T2 results greatly improve pathologic interpretation compared with that provided by peak-area ratios. The putative neurochemical roles of Lac, NAA, Cho, and Cr have been discussed previously. Briefly, the elevated levels of brain Lac following transient hypoxia-ischemia are thought to be due to overproduction and/or underutilization of Lac or a change in cellular redox equilibrium in the tissue itself.<sup>18–20</sup> Following perinatal hypoxia-ischemia, cerebral blood flow is generally increased, brain pH<sub>i</sub> can be alkaline, and there is early postasphyxial hypermetabolism<sup>53</sup> followed by luxury perfusion in the subsequent weeks.<sup>54–56</sup> The elevated brain [Lac] seen in injured brain following hypoxia-ischemia is probably due to a disruption of the balance between cytosolic and mitochondrial ATP-producing metabolic pathways and up-regulation of cell membrane transporters. Near-infrared spectroscopy studies suggest a decrease in oxidized cytochrome c, increased tissue oxygenation, and diminished oxygen use after hypoxia-ischemia.<sup>57–59</sup> We speculate that the pathologic threshold for brain Lac lies between 3 and 4.4 mmol/kg wet weight (Table 4); however, a much larger study population is needed to give precise metabolite concentration sensitivities and specificities for outcome in neonatal encephalopathy.

NAA is considered a neuronal marker, because apart from its presence in oligodendrocyte type 2A (O-2A) progenitors and, to a lesser extent, in immature oligodendrocytes,<sup>60</sup> NAA is primarily neuronal. A reduction in NAA is related to a reduction in neuronal/axonal attenuation and viability. However, because some reversibility in NAA peak-area ratios has been observed,<sup>61</sup> it may be possible to use NAA as a marker to monitor the effects of neuroprotection or neurogenesis. Combined with the possibility of decreased neuronal attenuation from reduced NAA concentrations, the prolonged T2 implies that a proportion of the remaining intact neurons have impaired ATP generation and viability.<sup>28,29</sup>

Cho is essential in normal cell function and directly affects nerve signaling (via acetylcholine), cell signaling, lipid transport, and cell membrane metabolism.<sup>62–64</sup> The Cho peak reflects total brain choline stores (mainly glycerophosphocholine and phosphocholine) but also has contributions from phosphoethanolamine (PEt) and ethanolamine. Cho is a putative marker of cellularity and cell turnover,<sup>65</sup> and reduced [Cho] may be associated with delayed myelination,<sup>66</sup> altered populations of cell types, decreased cellularity,<sup>67</sup> or apoptosis.<sup>68–71</sup>

The Cr peak comprises signals from creatine and PCr and, to a much lesser degree,  $\gamma$ -aminobutyric acid, lysine, and glutathione. PCr maintains energy-dependent systems in brain cells by buffering and conserving levels of ATP and adenosine diphosphate. Reduced [Cr] in the neonatal encephalopathy groups may reflect reduced overall cellularity; the increase in

Cr T2 observed in severe neonatal encephalopathy is discussed previously.

## Conclusions

Our results suggest that the most important prognostic MR spectroscopy indices in neonatal encephalopathy are metabolite concentrations, in particular [NAA]. Indeed, the only measurable that demonstrated a difference among all 3 groups (control, normal/mild, severe/fatal outcome) was [NAA]—the progressive reduction in [NAA] with outcome severity suggests that neuronal attenuation and viability decline with worsening outcome. Metabolite peak-area ratios are more useful prognostic indicators than concentration ratios because they depend on metabolite concentrations and T2 relaxation, both of which are pathologically modulated—metabolite concentration ratios depend only on the concentrations of the constituent metabolites. The observed changes in metabolite concentrations and T2 values also suggest that simple interpretation of peak-area ratios needs caution because Cr, in particular, is not a stable reference. Increases in metabolite T2 values may relate to impaired cellular energy production, failure of membrane pumps, and increased intracellular water. The increase in Cr T2 may have resulted from both increased intracellular water and phosphocreatine hydrolysis, leading to increased Cr, the latter having a longer T2 than phosphocreatine. Therefore, Cr T2 may constitute an indirect index of cellular energetics. Our recommendation is to acquire data that enable calculation of brain metabolite concentrations. However, if time constraints make this procedure impossible, metabolite peak-area ratios provide the next best method of assigning prognosis in neonatal encephalopathy.

## References

- Cowan F, Rutherford M, Groenendaal F, et al. Origin and timing of brain lesions in term infants with neonatal encephalopathy. *Lancet* 2003;361:736–42
- Thornberg E, Thringer K, Odeback A, et al. Birth asphyxia: incidence, clinical course and outcome in a Swedish population. *Acta Paediatr* 1995;84:927–32
- Badawi N, Kurinczuk JJ, Keogh JM, et al. Antepartum risk factors for newborn encephalopathy: the Western Australian case-control study. *BMJ* 1998;317:1549–53
- Azzopardi D, Wyatt JS, Cady EB, et al. Prognosis of newborn infants with hypoxic-ischemic brain injury assessed by phosphorus magnetic resonance spectroscopy. *Pediatr Res* 1989;25:445–51
- Groenendaal F, Veenhoven RH, van der Grond J, et al. Cerebral lactate and N-acetyl-aspartate/choline ratios in asphyxiated full-term neonates demonstrated in vivo using proton magnetic resonance spectroscopy. *Pediatr Res* 1994;35:148–51
- Hanrahan JD, Sargentoni J, Azzopardi D, et al. Cerebral metabolism within 18 hours of birth asphyxia: a proton magnetic resonance spectroscopy study. *Pediatr Res* 1996;39:584–90
- Martin E, Buchli R, Ritter S, et al. Diagnostic and prognostic value of cerebral 31P magnetic resonance spectroscopy in neonates with perinatal asphyxia. *Pediatr Res* 1996;40:749–58
- Penrice J, Cady EB, Lorek A, et al. Proton magnetic resonance spectroscopy of the brain in normal preterm and term infants, and early changes after perinatal hypoxia-ischemia. *Pediatr Res* 1996;40:6–14
- Amess PN, Penrice J, Wylezinska M, et al. Early brain proton magnetic resonance spectroscopy and neonatal neurology related to neurodevelopmental outcome at 1 year in term infants following presumed hypoxic-ischaemic brain injury. *Dev Med Child Neurol* 1999;41:436–45
- Barkovich AJ, Baranski K, Vigneron D, et al. Proton MR spectroscopy for the evaluation of brain injury in asphyxiated term neonates. *AJNR Am J Neuroradiol* 1999;20:1399–405
- Hanrahan JD, Cox IJ, Azzopardi D, et al. Relation between proton magnetic resonance spectroscopy within 18 hours of birth asphyxia and neurodevelopment at 1 year of age. *Dev Med Child Neurol* 1999;41:76–82
- Robertson NJ, Cox IJ, Cowan FM, et al. Cerebral intracellular lactic alkalosis

persisting months after NE measured by magnetic resonance spectroscopy. *Pediatr Res* 1999;46:287–96

- Robertson NJ, Kuint J, Counsell SJ, et al. Characterization of cerebral white matter damage in preterm infants using 1H and 31P MRS. *J Cereb Blood Flow Metab* 2000;20:1446–56
- Robertson NJ, Cowan FM, Cox IJ, et al. Brain alkaline intracellular pH after neonatal encephalopathy. *Ann Neurol* 2002;52:732–42
- Lorek A, Takei Y, Cady EB, et al. Delayed (“secondary”) cerebral energy failure after acute hypoxia-ischemia in the newborn piglet: continuous 48-hour studies by phosphorus magnetic resonance spectroscopy. *Pediatr Res* 1994;36:699–706
- Mehmet H, Yue X, Penrice J, et al. Relation of impaired energy metabolism to apoptosis and necrosis following transient cerebral hypoxia-ischaemia. *Cell Death Differ* 1998;5:321–29
- Thoresen M, Penrice J, Lorek A, et al. Mild hypothermia after severe transient hypoxia-ischemia ameliorates delayed cerebral energy failure in the newborn piglet. *Pediatr Res* 1995;37:667–70
- Lei H, Peeling J. Effect of temperature on the kinetics of lactate production and clearance in a rat model of forebrain ischemia. *Biochem Cell Biol* 1998;76:503–09
- Penrice J, Lorek A, Cady EB, et al. Proton magnetic resonance spectroscopy of the brain during acute hypoxia-ischemia and delayed cerebral energy failure in the newborn piglet. *Pediatr Res* 1997;41:795–802
- Rothman DL, Howseman AM, Graham GD, et al. Localized proton NMR observation of [3–13C] lactate in stroke after [1–13C] glucose infusion. *Magn Reson Med* 1991;21:302–07
- Zarifi MK, Astrakas MG, Poussaint TY, et al. Prediction of adverse outcome with cerebral lactate level and apparent diffusion coefficient in infants with perinatal asphyxia. *Radiology*. 2002;225:859–70
- Fan G, Wu Z, Chen L, et al. Hypoxia-ischemic encephalopathy in full-term neonate: correlation proton MR spectroscopy with MR imaging. *Eur J Radiol* 2003;45:91–98
- Miller SP, Newton N, Ferriero DM, et al. Predictors of 30-month outcome after perinatal depression: role of proton MRS and socioeconomic factors. *Pediatr Res* 2002;52:71–77
- Barkovich AJ, Westmark KD, Bedi HS, et al. Proton spectroscopy and diffusion imaging in the first day of life after perinatal asphyxia: preliminary report. *AJNR Am J Neuroradiol* 2001;22:1786–94
- Soul JS, Robertson RL, Tzika AA, et al. Time course of changes in diffusion-weighted magnetic resonance imaging in a case of neonatal encephalopathy with defined onset and duration of hypoxic-ischemic insult. *Pediatrics* 2001;108:1211–14
- Hanrahan JD, Cox IJ, Edwards AD, et al. Persistent increases in cerebral lactate concentration after birth asphyxia. *Pediatr Res* 1998;44:304–11
- Groenendaal F, van der Grond J, Witkamp TD, et al. Proton magnetic resonance spectroscopic imaging in neonatal stroke. *Neuropediatrics* 1995;26:243–48
- Cady EB, Lorek A, Penrice J, et al. Brain-metabolite transverse relaxation times in magnetic resonance spectroscopy increase as adenosine triphosphate depletes during secondary energy failure following acute hypoxia-ischaemia in the newborn piglet. *Neurosci Lett* 1994;182:201–04
- Cady EB. Metabolite concentrations and relaxation in perinatal cerebral hypoxia-ischaemia injury. *Neurochem Res* 1996;21:1043–52
- Yang KE, Cohen BM, Hirashima F, et al. Phosphocreatine Has Shorter T2\* Than Creatine in Vivo: Proceedings of the Ninth Annual Meeting of the International Society of Magnetic Resonance in Medicine (ISMRM). April 21–27 2001. Glasgow, Scotland, UK; 2001:213
- Hüppi P, Fusch C, Boesch C, et al. Regional metabolic assessment of human brain during development by proton magnetic resonance spectroscopy in vivo and by high performance liquid chromatography/gas chromatography in autopsy tissue. *Pediatr Res* 1995;37:145–50
- Hüppi P, Posse S, Lazeyras F, et al. Magnetic resonance in preterm and term newborns: 1H-spectroscopy in developing human brain. *Pediatr Res* 1991;30:574–78
- Kreis R, Ernst T, Ross B. Absolute quantitation of water and metabolites in the human brain. Part II. Metabolite concentrations. *J Magn Reson* 1993;102:9–19
- Pouwels P, Brockman K, Kruse B, et al. Regional age dependence of human brain metabolites from infancy to adulthood as detected by quantitative localized proton MRS. *Pediatr Res* 1999;46:474–85
- Cady EB, Penrice J, Amess PN, et al. Lactate, N-acetylaspartate, choline and creatine concentrations, and spin-spin relaxation in thalamic and occipitoparietal regions of developing human brain. *Magn Reson Med* 1996;36:878–86
- Sarnat HB, Sarnat MS. Neonatal encephalopathy following fetal distress: a clinical and electroencephalographic study. *Arch Neurol* 1976;33:696–705
- Amiel-Tison C. Clinical assessment of the infant nervous system. In: Levene MI, Lilford RJ, eds. *Fetal and Neonatal Neurology and Neurosurgery*. 2nd ed. London, UK: Churchill Livingstone; 1995:83–104
- Griffiths R. *The Abilities of Babies*. Amersham, UK: Association for Research in Infant and Child Development; 1996 (revision)
- Cady EB. Quantitative combined phosphorus and proton PRESS of the brains of newborn human infants. *Magn Reson Med* 1995;33:557–63

40. Kittel C. *Introduction to Solid State Physics*. 3rd ed. London, UK: Wiley; 1968: 516–17
41. Vanhamme L, van den Boogart A, van Huffel S. Improved method for accurate and efficient quantification of MRS data with use of prior knowledge. *J Magn Reson* 1997;129:35–43
42. Kingsley PB. Scalar coupling and zero-quantum coherence relaxation in STEAM: implications for spectral editing of lactate. *Magn Reson Med* 1994;31: 315–19
43. Yablonsky DA, Neil JJ, Raichle ME, et al. Homonuclear J coupling effects in volume localized NMR spectroscopy: pitfalls and solutions. *Magn Reson Med* 1998;39:169–78
44. Dobbing J, Sands J. Quantitative growth and development of human brain. *Arch Dis Child* 1973;48:757–67
45. van der Toorn A, Dijkhuizen RM, Tulleken CA, et al. T1 and T2 relaxation times of the major 1H-containing metabolites in rat brain after focal ischemia. *NMR Biomed* 1995;8:245–52
46. Rumpel H, Nedelcu J, Aguzzi A, et al. Late glial swelling after acute cerebral hypoxia-ischemia in the neonatal rat: a combined magnetic resonance and histochemical study. *Pediatr Res* 1997;42:54–59
47. Dugan LL, Choi DW. Hypoxic-ischemic brain injury and oxidative stress. In: Siegel GJ, Agranoff BW, Albers RW, et al, eds. *Basic Neurochemistry: Molecular, Cellular and Medical aspects*, 6th ed. Philadelphia, Pa: Lippincott-Raven Publishers; 1999;711–30
48. Nicholson JK, Timbrell JA, Bales JR, et al. A high-resolution proton nuclear magnetic resonance approach to the study of hepatocyte and drug metabolism. *Mol Pharmacol* 1985;27:634–43
49. Altman PL, Dittmer DS. *Biological Handbooks, Blood and Other Body Fluids*. Washington, DC: Federation of American Society for Experimental Biology; 1961:315–16
50. Diem K, Lentner C. *Scientific Tables*. 7th ed. Basle, Switzerland: CIBA-GEIGY; 1970:635–40
51. McGale EHF, Pye IF, Stonier C, et al. Studies of the inter-relationship between cerebrospinal fluid and plasma amino acid concentrations in normal individuals. *J Neurochem* 1977;29:291–97
52. Cady EB, Amess P, Penrice J, et al. Early cerebral-metabolite quantification in perinatal hypoxic-ischaemic encephalopathy by proton and phosphorus magnetic resonance spectroscopy. *Magn Reson Imaging* 1997;15:605–11
53. Syrota A, Castaing M, Rougemont D, et al. Tissue acid-base balance and oxygen metabolism in human cerebral infarction studied with positron emission tomography. *Ann Neurol* 1983;14:419–28
54. Syrota A, Samson Y, Boullais C, et al. Tomographic mapping of brain intracellular pH and extracellular water space in stroke patients. *J Cereb Blood Flow Metab* 1985;5:358–68
55. Hakim AM, Pokrupa RP, Villanueva J, et al. The effect of spontaneous reperfusion on metabolic function in early human cerebral infarcts. *Ann Neurol* 1987;21:279–89
56. Fidelman ML, Seeholzer SH, Walsh KB, et al. Intracellular pH mediates action of insulin on glycolysis in frog skeletal muscle. *Am J Physiol* 1982;242:C87–93
57. van Bel F, Dorrepaal CA, Benders MJ, et al. Changes in cerebral hemodynamics and oxygenation in the first 24 hours after birth asphyxia. *Pediatrics* 1993;92: 365–72
58. Geron TJ, Kane NM, Manara AR, et al. Near-infrared spectroscopy in adults: effects of extracranial ischaemia and intracranial hypoxia on estimation of cerebral oxygenation. *Br J Anaesth* 1994;73:503–06
59. Marks N, Berg MJ. Recent advances on neuronal caspases in development and neurodegeneration. *Neurochem Int* 1999;35:195–220
60. Urenjak J, Williams SR, Gadian DG, et al. Specific expression of N-acetylaspartate in neurons, oligodendrocyte-type-2 astrocyte progenitors and immature oligodendrocytes in vitro. *J Neurochem* 1992;59:55–61
61. Jagannathan NR, Tandon N, Raghunathan P, et al. Reversal of abnormalities of myelination by thyroxine therapy in congenital hypothyroidism: localized in vivo proton magnetic resonance spectroscopy (MRS) study. *Brain Res Dev Brain Res* 1998;109:179–86
62. Zeisel SH. Dietary choline: biochemistry, physiology and pharmacology. *Annu Rev Nutr* 1981;1:95–121
63. Zeisel SH. Choline: needed for normal development of memory. *J Am Coll Nutr* 2000;19[suppl]:528S–531S
64. Exton JH. Phosphatidylcholine breakdown and signal transduction. *Biochem Biophys Acta* 1994;1212:26–42
65. Miller BL, Chang L, Booth R, et al. In vivo <sup>1</sup>H MRS choline: correlation with in vitro chemistry/histology. *Life Sciences* 1996;58:1929–35
66. Alkan A, Kutlu R, Yakinci C, et al. Delayed myelination in a rhizomelic chondrodysplasia punctata case: MR spectroscopy findings. *Magn Reson Imaging* 2003;21:77–80
67. Roelants-Van Rijn AM, van der Grond J, de Vries LS, et al. Value of (1)H-MRS using different echo times in neonates with cerebral hypoxia-ischemia. *Pediatr Res* 2001;49:356–62
68. Yen CL, Mar MH, Meeker RB, et al. Choline deficiency induces apoptosis in primary cultures of fetal neurons. *FASEB J* 2001;15:1704–10
69. Albright CD, Tsai AY, Friedrich CB, et al. Choline availability alters embryonic development of the hippocampus and septum in the rat. *Brain Res Dev Brain Res* 1999;113:13–20
70. Holmes-McNary MQ, Loy R, Mar MH, et al. Apoptosis is induced by choline deficiency in fetal brain and in PC12 cells. *Brain Res Dev Brain Res* 1997;101: 9–16
71. Yen CL, Mar MH, Zeisel SH. Choline deficiency-induced apoptosis in PC12 cells is associated with diminished membrane phosphatidylcholine and sphingomyelin, accumulation of ceramide and diacylglycerol, and activation of a caspase. *FASEB J* 1999;13:135–42